International Journal of Electrical and Electronics Engineers
Vol. No.8 Issue 02, July-December 2016
ISSN (O) 2321-2055
ISSN (P) 2321 -2045

SIMULATION OF SLIDING MODE OBSERVER FOR SENSORLESS CONTROL OF BLDC MOTOR

Y. Santosh Kumar[1], P. Devendra[2]

[1]PG student, Department of EEE, GMR Institute of Technology, Rajam, (India)

[2]Associate Professor, Department of EEE, GMR Institute of Technology, Rajam, (India)

ABSTRACT

The BLDC Motor (BLDCM) is used as a drive because of its features which are far better than other motors. The BLDCM controlled through electronic commutation with reference to rotor position using hall sensors. But hall sensors are unreliable in harsh environment. So the sensorless technique is good choice in these harsh situations as rotor position estimated using only quantities measured from supply terminals. In the closed loop sensorless techniques, reduced order observers are much simpler in which an internal correction mechanism in motor model is used for position estimation. One of above techniques is, sliding mode observer (SMO). The control scheme design for BLDC Motor mainly focussed to control the inverter i.e. by electronic commutation. In practice, the design of the BLDCM drive involves modelling, devise of control scheme, simulation and parameter tuning. The hysteresis controller is one of efficient control schemes due to its ease in design and simple structure. This paper proposes a control technique using hysteresis current controller in conjunction with SMO.

***Keywords:* BLDC Motor, Sensorless Methods, Sliding Mode Observer, Hysteresis Current Controller**

I. INTRODUCTION

BLDCM in recent years widely preferred due to possession of characteristics like energy efficiency, less power consumption and simple control and being a cheaper solution for a wide range of applications. The BLDCM is consists of armature winding that placed in stator and permanent magnets placed in rotor. For the motor control, electronic commutation through the inverter is used which eliminates the brush and the commutator arrangement. Armature winding on the stator has the benefit of dissipating the heat from windings easily with effective cooling arrangement [1]. In poly phase BLDCM, to conduct a phase, exact location of the rotor poles needed. And the switching sequence must have a phase difference of 90^0 between stator and rotor fluxes to get maximum torque [2]. The phase winding will be given excitation only if a rotor pole is in its vicinity. In BLDCM, it is easy to sense the position of rotor as the armature is concentrated winding in nature. In a three phase BLDCM, two out of three phases are in conduction at any time which explains firing sequence changes for every 60^0 electrical and the need of position of rotor sensing at discrete intervals [3].

Hall sensors or variable reluctance (VR) sensors are useful for sensing of position of rotor. The hall sensor which is placed on non-rotating part of motor transmits signal based on proximity of a pole as the magnetic field of rotor induces emf in it. In case of a three phase BLDCM, three sensors are placed with a phase shift 120^0 to get that information [3]. A VR sensor contains an iron tooth gear attached to the rotor shaft. As the rotor rotates, there will be a change in flux due to uneven air gap which induces an emf in the coil of the sensor. This tooth gear consist a gap in outer portion to provide discontinuity in the generated waveform. This signal transmitted to the controller to generate switching sequence [4].

For the position sensing, position sensors are mounted on the motor and need separate electronic circuitry and a cabling system for signal transmission [5]. These arrangements are costly and decrease reliability. So these schemes cannot be used where high reliability required in harsh environment. One solution is to estimate the position with the help of measured electrical quantities and that's why called as sensorless control. It is also useful as a backup scheme. Sensorless control uses terminal voltages and currents information for position estimation using sensorless algorithms [5]. These signals may be injected either at fundamental frequency or high frequency [6]. In some of the fundamental excitation methods, position and speed information is estimated using back emf voltages. The principle of direct emf sensing is, whenever only two of the three phases are conducting, non-conducting phase carry only the back emf which is useful for position sensing. As this information contains noise, filters are essential in reducing harmonics. The zero crossing of the back emf does not directly useful for commutation and there must be a phase shift in switching signals. These limitations not present in case of indirect back emf sensing methods like voltage integration method or terminal current sensing method [7].

In open loop sensorless methods, the position information is attained by terminal voltages sensing without any correction mechanism and this method is sensitive to variations in parameters [8]. In close loop methods, observers are preferable because they use internal correction mechanism for accuracy. Observers may be a full order or reduced order observer. Full order observers contain both electrical and mechanical models thus complex in nature whereas reduced order observer have only electrical model is required for position estimation which is much simpler than former [9]. Reduced order observers categorised as flux observers and current observers. In flux observer, a magnetic model is used as the reference model and in reduced order current observer uses electrical model in which the rotor position attained by estimating the back emf voltages [5]. One of reduced order current observer techniques is sliding mode observer (SMO) which estimates the rotor speed and its integration gives rotor position [10].

BLDCM as a drive is easy to control with negligible maintenance. This motor controlled with electronic commutation using a controller to get optimal performance. In such, current controlled voltage source inverters are preferred for their faster response and accuracy. One option is to use hysteresis current controller. Hysteresis-band PWM is basically an instantaneous feedback current control method of PWM where the actual current continually tracks the command current within hysteresis-band. The control circuit generates a reference signal using the error in input and it is compared with the actual signal. If the actual signal exceeds or drops below the hysteresis band limit, the switching sequence is generated to limit the actual current within the band limit [14].

This paper deals with a sensorless speed control scheme of BLDC with rotor position estimated with SMO. In this paper, based on the mathematical modelling of BLDC motor, SMO is designed to estimate the rotor position and speed. Then hysteresis controller is implemented to control the inverter for the optimum performance of motor. The model is simulated using MATLAB/SIMULINK and the simulation results have been validated to prove its effectiveness.

The mathematical modelling of BLDC motor is presented in section 2. The SMO for the following motor is designed in the section 3. Hysteresis current controller for the same drive is implemented in the section 4. The control scheme using hysteresis current controller in conjunction with SMO is and the simulation results of the proposed scheme are presented in section 5. Finally the proposed scheme is concluded in section 6.

II. MATHEMATICAL MODEL OF PM BLDC MOTOR

The electrical circuit modelling equations for a three phase BLDCM are derived in terms of phase variables denoted with the sequence *abc* [11].

The KVL equation for the phase *a* is:

$$V_a = R_s i_a + L\frac{di_a}{dt} + e_a \tag{1}$$

The state equation for above expression is:

$$\frac{di_a}{dt} = \frac{1}{L}V_a - \frac{R_s}{L}i_a - \frac{1}{L}e_a \tag{2}$$

Where $L = L_s - M$ is the phase stator inductance, R is phase stator resistance, e_a is induced back emf, V_a is the phase voltage and i_a is the state variable for the phase *a*.

The induced back emf is:

$$e_a = k_b f_a(\theta_r)\omega_r \tag{3}$$

Where k_b is back emf constant, $f_a(\theta_r)$ is a unit function generator as a function of rotor position for the phase a, θ_r is the rotor electrical position and ω_r is the rotor electrical speed.

And $f_a(\theta_r)$ is given by:

$$f_a(\theta_r) = \begin{cases} (\theta_r)\frac{6}{\pi}, & 0 < \theta_r < \frac{\pi}{6} \\ 1, & \frac{\pi}{6} < \theta_r < \frac{5\pi}{6} \\ (\pi - \theta_r)\frac{6}{\pi}, & \frac{5\pi}{6} < \theta_r < \frac{7\pi}{6} \\ -1, & \frac{7\pi}{6} < \theta_r < \frac{11\pi}{6} \\ (\theta_r - 2\pi)\frac{6}{\pi}, & \frac{11\pi}{6} < \theta_r < 2\pi \end{cases} \tag{4}$$

The unit function generators and the voltage equations for other phases for the other phases are equal but only differ in phase shift of 120^0 with each.

The electromechanical equation with the load torque is:

$$J\frac{d\omega_m}{dt}+B\omega_m=T_e-T_l \tag{5}$$

Where J is moment of inertia, B is frictional coefficient, T_l is load torque and T_e is electromagnetic torque.

The state equation for the speed with rotor speed as state variable is given by:

$$\frac{d\omega_m}{dt}=\frac{1}{J}T_e-\frac{1}{J}T_l-\frac{B}{J}\omega_m \tag{6}$$

The rotor position calculated from the rotor speed as:

$$\frac{d\theta_r}{dt}=\frac{p}{2}\omega_m \tag{7}$$

Where p is the number of poles.

The electromagnetic torque is obtained as:

$$T_e=(e_a i_a+e_b i_b+e_c i_c)/\omega_m \tag{8}$$

Fig. 1 shows the complete mathematical model of BLDC motor with open loop control where the firing sequence is generated with the rotor position obtained directly from motor.

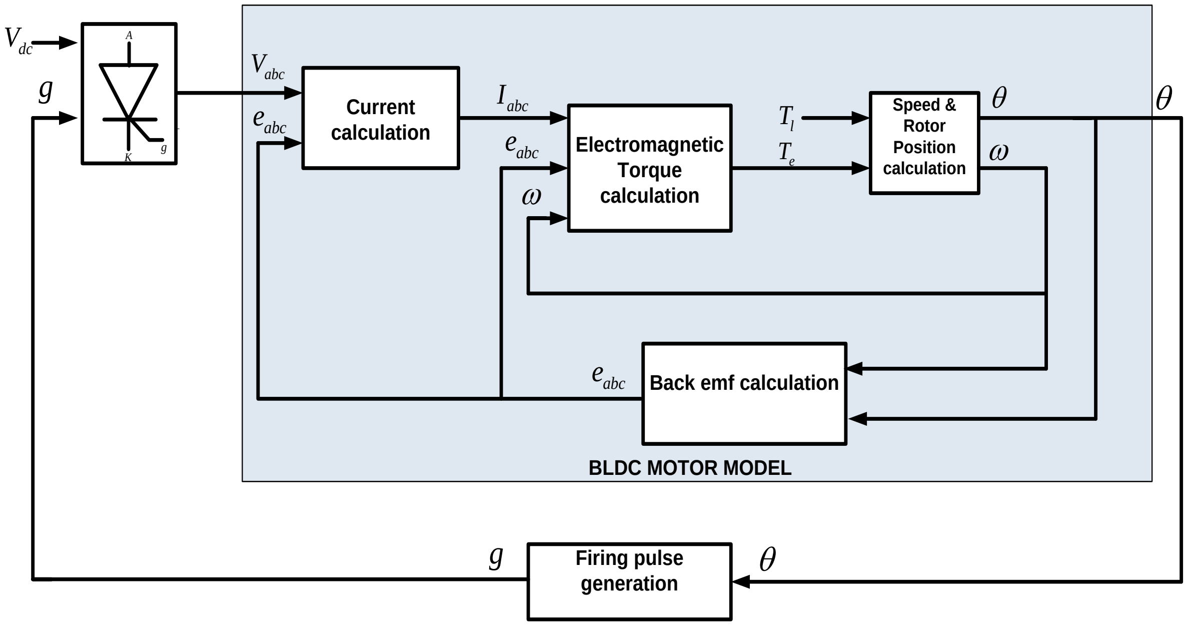

Fig. 1. Mathematical model of BLDC motor with open loop control

III. SLIDING MODE OBSERVER

Sliding mode observer is a reduced order current observer in which the terminal currents are the reference outputs and the adaptive model estimates motor currents. The error between estimated and actual currents is sent to the adaptive model to estimate the back emf [13].

The current state equation for the phase *a* is:

$$\frac{di_a}{dt}=\frac{1}{L}V_a-\frac{R_s}{L}i_a-\frac{1}{L}e_a \tag{10}$$

The sliding mode technique should ensure that the value of estimated parameter must slides along with that of actual parameter. The sliding mode equations for back emf estimation for the phase *a* is:

$$\frac{d\hat{i}_a}{dt} = \frac{1}{L}V_a - \frac{R_s}{L}\hat{i}_a - \frac{1}{L}\hat{e}_a + k_{11}\,\mathrm{sat}(\tilde{i}_a) \quad (11)$$

$$\frac{d\hat{e}_a}{dt} = k_{21}\,\mathrm{sat}(\tilde{i}_a) \quad (12)$$

Where $\hat{i}_a$, $\hat{e}_a$ are the estimated values of phase current and back emf respectively and $\tilde{i}_a = i_a - \hat{i}_a$ is the sliding surface which represents the error between actual and estimated currents.

The dynamic equation for $\tilde{i}_a$ is:

$$\tilde{i}'_a = -\frac{1}{L_L}\hat{e}_a - k_{11}sat(\tilde{i}_a) \quad (13)$$

The signum function for $\tilde{i}_a$ is:

$$sign(\tilde{i}_a) = \begin{cases} 1; & \tilde{i}_a > 0 \\ 0; & \tilde{i}_a = 0 \\ -1; & \tilde{i}_a < 0 \end{cases} \quad (14)$$

The chattering effect can be eliminated using saturation function which defined as:

$$sat(\tilde{i}_a) = \begin{cases} \frac{|\tilde{i}_a|}{\varepsilon}; & |\tilde{i}_a| \le \varepsilon \\ sign(\tilde{i}_a); & |\tilde{i}_a| > \varepsilon \end{cases} \quad (15)$$

Where ε is the sliding surface band.

The sliding surface becomes zero when both actual and estimated currents are equal. To ensure convergence, the observer gains proper selection of *a1* and a_2 needed which can be attained with the help of a stability theorem [13].

The candidate Lyapunov function for SMO is considered as:

$$V(\tilde{i}) = \frac{1}{2}(\tilde{i}_a^{\,2} + \tilde{i}_b^{\,2} + \tilde{i}_c^{\,2}) \quad (16)$$

The derivative of $V(\tilde{i})$ with respect to time given as:

$$V'(\tilde{i}) = \tilde{i}'_a\tilde{i}_a + \tilde{i}'_b\tilde{i}_b + \tilde{i}'_c\tilde{i}_c \quad (17)$$

$$V'(\tilde{i}) = \tilde{i}_a(-\frac{1}{L_L}\hat{e}_a - k_{11}sat(\tilde{i}_a)) + \tilde{i}_b(-\frac{1}{L_L}\hat{e}_b - k_{12}sat(\tilde{i}_b)) + \tilde{i}_c(-\frac{1}{L_L}\hat{e}_c - k_{13}sat(\tilde{i}_c)) \quad (18)$$

To ensure convergence $V'(\tilde{i}) < 0$ and the observer gains should satisfy the following conditions:

$$\begin{aligned} &if \quad \tilde{i}_a > 0; \quad gain \quad k_{11} > -\frac{1}{L}e_{a-\max} \\ &if \quad \tilde{i}_a < 0; \quad gain \quad k_{11} > \frac{1}{L}e_{a-\max} \end{aligned} \quad (19)$$

The above relations are similar for the *b, c* phases. So the observer gain values for all the lines chosen such that:

International Journal of Electrical and Electronics Engineers
Vol. No.8 Issue 02, July-December 2016
ISSN (O) 2321-2055
ISSN (P) 2321 -2045

$$a_1 > \frac{1}{L}|e|_{\max} \quad and \quad a_2 < 0 \tag{20}$$

Where $k_{11} = k_{12} = k_{13} = a_1$, $k_{21} = k_{22} = k_{23} = a_2$ and $e_{\max}$ is maximum value of line back emf.

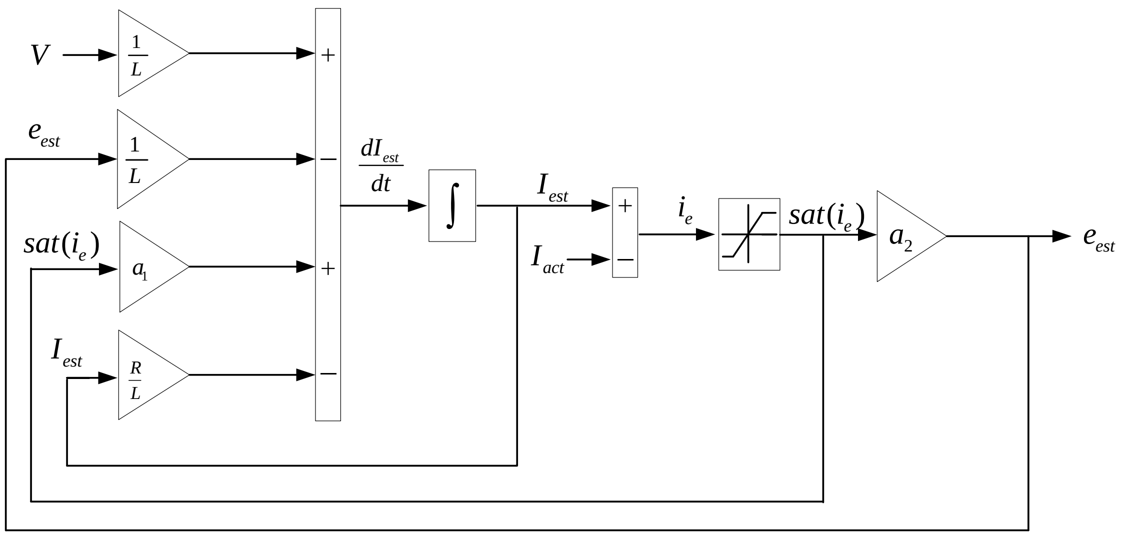

Fig. 2. Sliding mode observer

Fig. 2 represents a sliding mode observer for back emf estimation which is useful for rotor position estimation. The rotor speed is estimated as:

$$\hat{\omega}_r = \frac{1}{k_b}\sqrt{(\hat{e}_a{}^2 + \hat{e}_b{}^2 + \hat{e}_c{}^2)} \tag{21}$$

Where $\hat{\omega}_r$ is the rotor speed and k_b is the back emf constant.

The rotor position $\hat{\theta}_r$ is calculated as shown in Fig. 3 is:

$$\frac{d\hat{\theta}_r}{dt} = \hat{\omega}_r \tag{22}$$

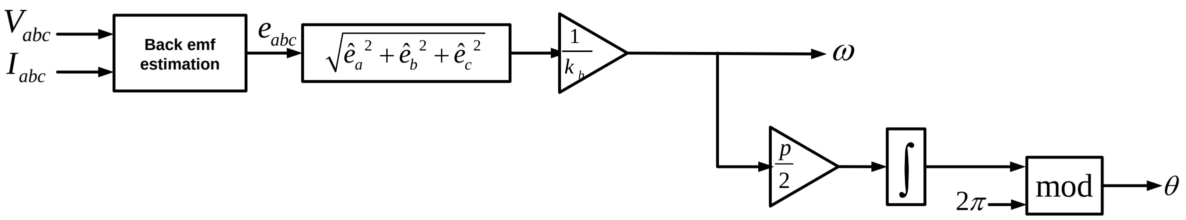

Fig. 3. Block diagram of speed and rotor position estimation

IV. HYSTERESIS CURRENT CONTROLLER

Hysteresis controller is the simple one in which a hysteresis band limit is defined for reference current and the phase current is ensured to follow the path of reference current in between hysteresis band. Hysteresis band consist of two limits i.e. Upper limit and Lower limit. The upper and lower bounds of the hysteresis band are set

International Journal of Electrical and Electronics Engineers
Vol. No.8 Issue 02, July-December 2016
ISSN (O) 2321-2055
ISSN (P) 2321 -2045

for the motor current, and the hysteresis controller logic control can be described according to the following rules. In a basic implementation of the hysteresis current controller, the switching signals are derived from the comparison of the current error with a fixed hysteresis band [14].

The reference current can be generated with the error in speed as:

$$i_{ref} = \frac{1}{k_t}\left(k_p + \frac{k_i}{s}\right)(\omega_{ref} - \omega) \tag{23}$$

The reference current for each phase can be generated using the function generator as:

$$\begin{array}{ll} Quadrant-I & Quadrant-IV \\ f_a(\theta_r) \geq 1; i_{aref} = i_{ref} & f_a(\theta_r) \leq -1; i_{aref} = -i_{ref} \\ f_b(\theta_r) \geq 1; i_{bref} = i_{ref} & f_b(\theta_r) \leq -1; i_{bref} = -i_{ref} \\ f_c(\theta_r) \geq 1; i_{cref} = i_{ref} & f_c(\theta_r) \leq -1; i_{cref} = -i_{ref} \end{array} \tag{24}$$

The load currents are sensed and compared with the respective command currents using three independent hysteresis comparators having a hysteresis band. The output signals of the comparators are used to active the inverter power switches as:

$$\begin{array}{lll} if & i_a < i_{a-ref} - h; & S_a = 1 \\ if & i_a > i_{a-ref} + h; & S_a = -1 \\ if & i_{a-ref} - h < i_a < i_{a-ref} + h; & and \\ & i_a < i_{a-ref}; & S_a = 1 \\ & i_a > i_{a-ref}; & S_a = -1 \end{array} \tag{25}$$

Where i_{a-ref} is the reference current for the phase *a* and S_a is the switching logic for phase *a*.

Fig. 4 represents diagrammatic representation of the hysteresis current controller used for a three phase inverter for BLDC motor.

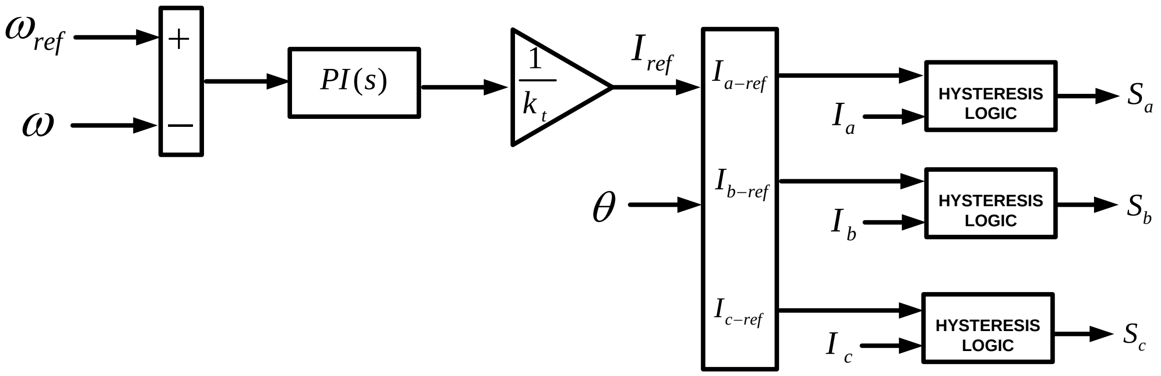

Fig. 4. Hysteresis current controller

In Fig. 4, load currents I_a, I_b and I_c are respectively forced to follow reference currents $I_{a\text{-}ref}$, $Ib_{\text{-}ref}$ and $I_{c\text{-}ref}$ within a hysteresis band by the switching action of the inverter.

V. SIMULATION RESULTS

BLDCM is simulated using MATLAB/SIMULINK with the specifications represented in the Table 1. The pictorial representation of speed control of BLDCM with SMO and hysteresis current controller shown in Fig. 5.

The proposed scheme is simulated using MATLAB/SIMULINK with the sliding mode parameters represented in Table 2.

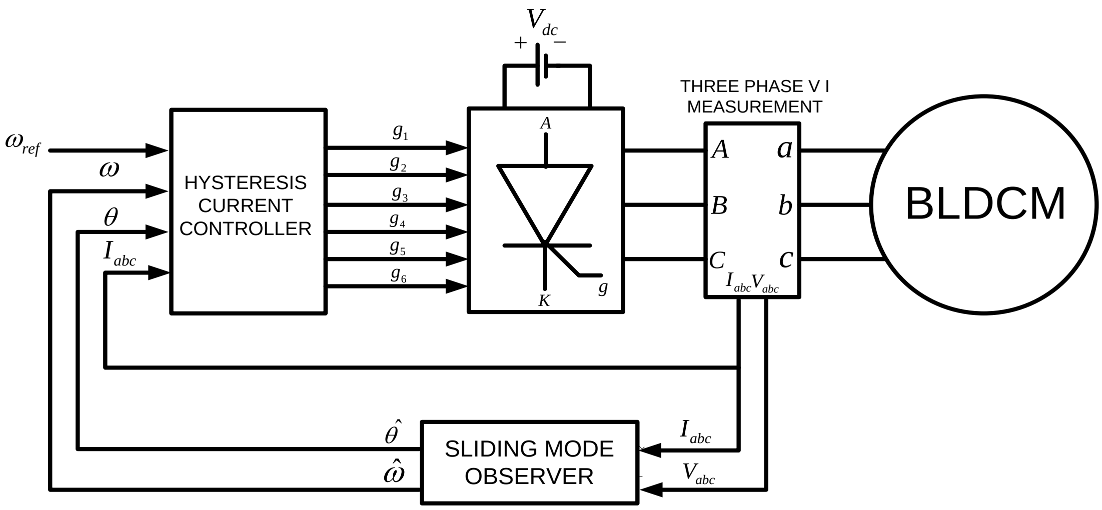

Fig. 5. Block diagram of sensorless control of BLDC motor with hysteresis controller with SMO

Table 1. BLDC motor parameters

Parameters	Symbol	Numerical value
Poles	P	4
Stator resistance (phase)	R_s	0.7 ohm
Stator self-inductance (phase)	L_s	1.72 mH
Mutual inductance (phase)	M	1.5 mH
Back emf constant	k_b	0.5128 V/(rad/sec)
Torque constant	k_t	0.049 N-m/A
Moment of inertia	J	0.0002 kg-m/s^2
Friction coefficient	B	0.002 N-m/rad/sec
DC link voltage	V_{dc}	160 V
Speed (base)	N	4000 rpm

Table 2. Sliding mode parameters

Gain	Numerical value
k_p	1
k_i	0.7
a_1	132000
a_2	-91000
ε	0.01

Fig. 6 represents the comparison of actual and estimated rotor positions and actual and estimated rotor speeds using SMO and hysteresis controller.

International Journal of Electrical and Electronics Engineers
Vol. No.8 Issue 02, July-December 2016
ISSN (O) 2321-2055
ISSN (P) 2321 -2045

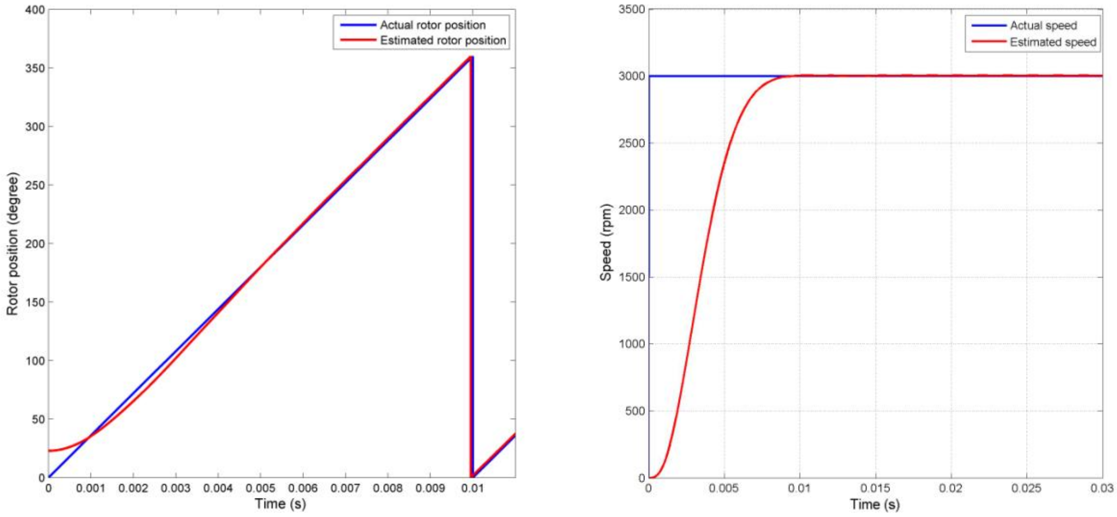

(a) (b)

Fig. 6. (a) Actual and estimated rotor positions (b) Actual and estimated rotor speeds

It is observed that the estimated rotor position has an error of 2^0 electrical from actual which is due to the delay because of filters. The sliding mode observer estimated the rotor speed with an initial delay of 0.01 sec and has an error of 1 rpm.

The proposed scheme is simulated under different speeds with a load torque of 0.3 N-m and 0.6 N-m applied at 1 sec and 2 sec respectively the results are shown in Fig. 7, Fig. 8 respectively.

At 400 rpm

Fig. 7 represents speed and torque curves obtained by the control of conventional hysteresis controller in conjunction with sliding mode observer with reference speed of 400 rpm respectively.

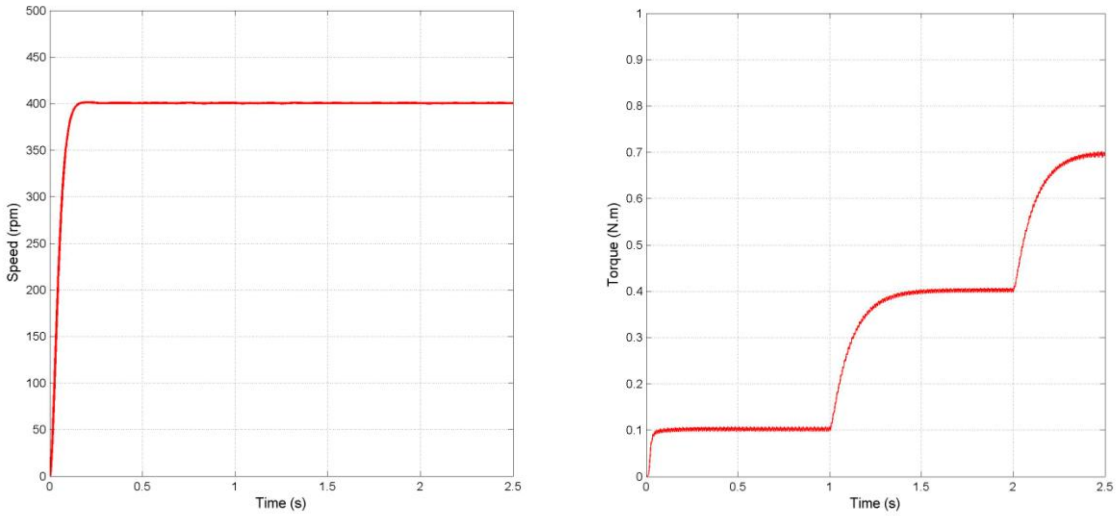

(a) (b)

Fig. 7. (a) Speed of Motor (b) Electromagnetic torque of Motor with SMO and hysteresis controller

The no-load torque is 0.11 N-m and the torque increased to 0.41 N-m at the load of 0.3 N-m at 1 sec and changed to 0.71 N-m at the load of 0.6 N-m applied at 2 sec.

At 2000 rpm

Fig. 9 represents speed and torque curves obtained by the control of conventional hysteresis controller in conjunction with sliding mode observer with reference speed of 2000 rpm respectively.

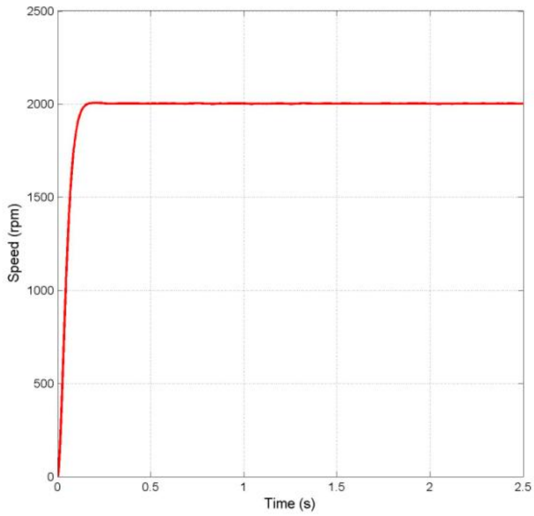

(a)

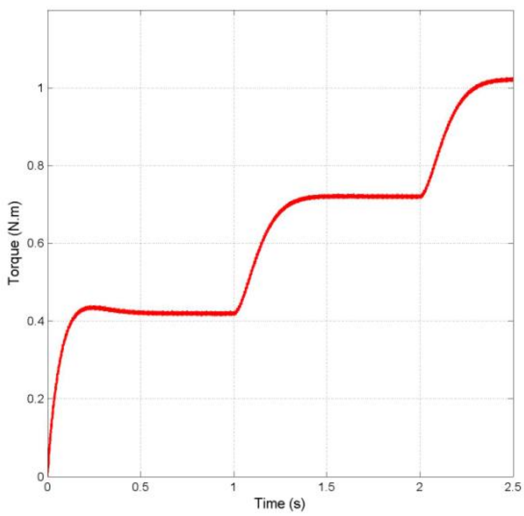

(b)

Fig. 8. (a) Speed of Motor (b) Electromagnetic torque of Motor with SMO and hysteresis controller

The no-load torque is 0.42 N-m and the torque increased to 0.72 N-m once the load of 0.3 N-m applied at 1 sec and to 1.1 N-m at 2 sec. From above graphs, we observed that the speed curve is smooth with a deviation of 0.1 rpm and torque ripple is well below 0.01 N-m.

VI. CONCLUSION

In this paper, a sensorless control of BLDCM using hysteresis current controller with SMO is proposed. The SMO is designed to estimate the rotor position without the help of the sensors. The estimated speed and rotor position using SMO compared with actual parameters of BLDCM and the results are accurate. The hysteresis current controller is implemented to control the inverter for better performance of the motor with the help of terminal currents, speed and rotor position. The proposed scheme accurately controlled the motor at desired speeds with lower torque ripple.

REFERENCES

[1] Hubik V., Sveda M., Singule V., On the Development of BLDC Motor Control Run-Up Algorithms for Aerospace Application, *Proceedings of the 13th Power Electronics and Motion Control Conference (EPE-PEMC 2008)*, Poznan, Poland, September 2008; pp. 1620-1624.

International Journal of Electrical and Electronics Engineers
Vol. No.8 Issue 02, July-December 2016
ISSN (O) 2321-2055
ISSN (P) 2321 -2045

[2] Paul P. Acarnley and J. F. Watson, Review of position-sensorless operation of brushless permanent-magnet machines, *IEEE Transactions on Industrial Electronics*, vol. 53, no. 2, pp. 352-362, April 2006.

[3] Gamazo-Real, José Carlos, Ernesto Vázquez-Sánchez, Jaime Gómez-Gil, Position and Speed Control of Brushless DC Motors Using Sensorless Techniques and Application Trends, *Sensors (Basel, Switzerland)* 10.7 (2010): 6901–6947. PMC. Web. 21 Apr. 2016.

[4] Bucak, Position Error Compensation via a Variable Reluctance Sensor Applied to a Hybrid Vehicle Electric Machine, *Sensors 2010*, 10, 1918-1934.

[5] F. Betin et al., Trends in Electrical Machines Control: Samples for Classical, Sensorless, and Fault Tolerant Techniques, *in IEEE Industrial Electronics Magazine*, vol. 8, no. 2, pp. 43-55, June 2014.

[6] J.C. Moreira, Indirect Sensing of Rotor Flux Position of Permanent Magnet AC Motors Operating Over a Wide Speed Range, *IEEE Tran. Ind. Applicat.*, vol. 32, no. 6, pp. 1394-1401,November/December 1996.

[7] N. Bianchi, S. Bolognani, J.H. Jang, and S.K. Sul, Advantages of Inset PM Machines for Zero-Speed Sensorless Position Detection, *IEEE Tran. Ind. Applicat*., vol. 44, no. 4, pp. 1190-1198, July/August2008.

[8] H.B. Wang, H.P. Liu, A novel sensorless control method for brushless DC motor, *IET Electric Power Applications.*, vol. 3, issue. 3, pp. 240-246, 2009.

[9] R. B. Sepe, J.H. Lang, Real-Time Observer-Based (Adaptive) Control of a Permanent-Magnet Synchronous Motor without Mechanical Sensors, *IEEE Tran. Ind. Applicat.*, vol. 28, no. 6, pp. 1345-1352, November/December 1992.

[10] Y.S. Han, J.S. Choi and, Y.S Kim, Sensorless PMSM Drive with a Sliding Mode Control Based Adaptive Speed and Stator Resistance Estimator, *IEEE Tran. Magn.*, vol. 36, no. 5, pp. 3588-3591,September 2000.

[11] R. Krishnan, Modelling, simulation and analysis of permanent magnet motor drives, PART II: The Brushless DC motor drive, P. Pillay and R. Krishnan, *IEEE Tran. Ind. Applicat*.,, vol.25, no.2, March/April 1989.

[12] R. Bojoi, M. Pastorelli, J. Bottomley, P. Giangrande and C. Gerada, Sensorless control of PM motor drives - A technology status review, *Electrical Machines Design Control and Diagnosis (WEMDCD)*, 2013 IEEE Workshop on, Paris, 2013, pp. 168-182.

[13] A. Deenadayalan and G. Saravana Ilango, Position sensorless sliding mode observer with sigmoid function for Brushless DC motor, *Advances in Power Conversion and Energy Technologies (APCET), 2012 International Conference on*, Mylavaram, Andhra Pradesh, 2012, pp. 1-6.

[14] E. M. Suhara and M. Nandakumar, Analysis of Hysteresis Current Control Techniques for Three Phase PWM Rectifiers, *International Conference on Signal Processing, Informatics, Communication and Energy Systems (SPICES)*, 2015 IEEE, pp. 1-5, 2015.